Seventh South African Conference on Computational and Applied Mechanics
SACAM10
Pretoria, 10–13 January 2010

Experimental development of an ultrasonic linear motor

G. M'Boungui[*,1], P.W. Loveday[*,2], C. Long[*,3]

Sensor Science and Technology, CSIR Materials Science and Manufacturing
PO Box 395, Pretoria, 0001, South Africa,
[1]GMBoungui@csir.co.za, [2]PLoveday@csir.co,za, [3]CLong@csir.co.za

Keywords: Lissajous Pattern, Piezoelectric Ultrasonic Motor

Abstract

We investigate a novel ultrasonic motor which generates a stator trajectory in the form of a figure-of-eight by superimposing two resonant modes, with one double the frequency of the other. Topology optimization was used to design the stator structure. In contrast to traditional travelling wave ultrasonic motors, which require two modes to be driven 90° out of phase, only one amplifier is required to drive the proposed device. A prototype device was characterised experimentally and was used to drive a linear bearing at 14 mm/s reversibly and a force of 50 mN was developed by the motor.

1 Introduction

Piezoelectric motors present, among other advantages the fact that they are not affected nor do they create a magnetic field, their design is simple using few parts, the holding torque they present is high, their operating speed is adjustable down to zero without the need for gearing, etc. when compared to the traditional electric motor [1][2]. Due to the increasing interest they present, we investigate a piezoelectric motor based on a resonator that has two natural modes with resonant frequency in an integer ratio. These two modes are excited to drive a particular point located on the resonator (stator) surface in a Lissajous pattern [3]. This particular point is used as the contact point between the vibrating surface of the resonator and a rotor (rotary motor) or slider (linear motor), which is pressed against the resonator. Friction forces during the intermittent contact between the stator and rotor or slider cause movement.
In this paper, measurements on a resonator, designed previously using topology optimisation [3] are presented in order to evaluate the resonator for use in a motor. First, the working principle is presented. After which the application of topology optimisation to design the stator structure is summarised, leading to a finite element mesh, used to analyse the device. From there, the stator free vibration characterization is conducted. Lastly, a motor prototype is realised and first trials of the structure characterization are presented.

2 Motor design and working principle

Traditionally, ultrasonic motors (USM) exploit the propagation of a travelling wave in a resonator (stator) and the friction intermittently created while in contact with an object (rotor) pressed against the resonator to drive this rotor as shown in Figure 1(a) [4]. The travelling wave comes from the superimposition of two standing waves whose phases differ by 90^0

from each other both in space and time. The trajectory of a contact point in this case is an ellipse. This requires the use of two electronic amplifiers. An alternate scheme, which uses only one amplifier, was demonstrated in [3]. In this case the resonator is designed to use two modes of vibration where the resonant frequency of the second mode is an integer multiple of the resonant frequency of the first mode. If the integer multiple is "2" then the figure-of-eight pattern shown in figure 1 (c) can be produced.
If we assume that one mode contributes motion in the *x* direction and the second mode motion in the *y* direction then Eq. (1) and (2) can be used to describe the trajectory of the contact point.

$$x = x_0 \sin(\omega t) \tag{1}$$

$$y = y_0 \sin(n\omega t + \varphi) \tag{2}$$

With ω the vibratory pulsation in rads^{-1}, φ, the phase difference between *x* and *y*, and *n*, a real number.

In particular, n=1 and $\varphi = \frac{\pi}{2}$ was used to generate the ellipse and $n = \frac{1}{2}$ and $\varphi = 0$ was used to generate the figure-of-eight pattern in figure 1 (c). The figure-of-eight pattern could also be generated with $\varphi = \pi$ and in this case the direction of motion would be reversed.

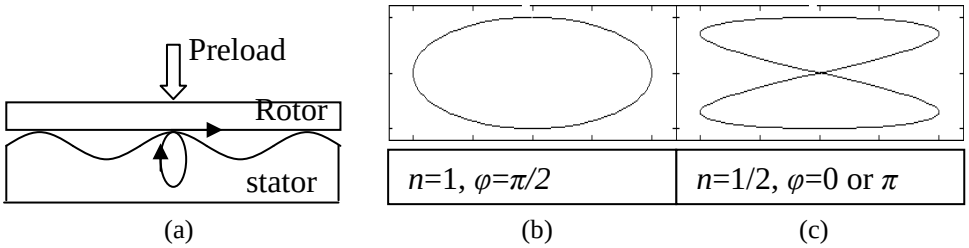

Figure 1: Ultrasonic motor working principle and contact point trajectories (a) driving principle for traditional motor with elliptical trajectory (b, c) output trajectories for case with n=1, $\varphi=\pi/2$ and n=1/2, φ=0 or π

3 Resonator design and motor setup

A resonator had been previously designed to have two modes with one resonant frequency being twice the other [5]. Topology optimization or material distribution method for finding the optimum lay-out of a linearly elastic structure was applied to achieve the predetermined resonant frequency ratio with the two corresponding modes (a flexural and a longitudinal one) usable to drive the contact point. The design space was descretized by finite elements and the amount of material in each element allowed to vary between 0 (void) and 1 (solid). The techniques developed for the minimum compliance problem were adapted and extended for this specific case to tackle structural design problems including free and forced vibration problems [5].

Figure 2 shows a detailed finite element mesh used to analyse the device and the deformation of the structure for the two expected modes.

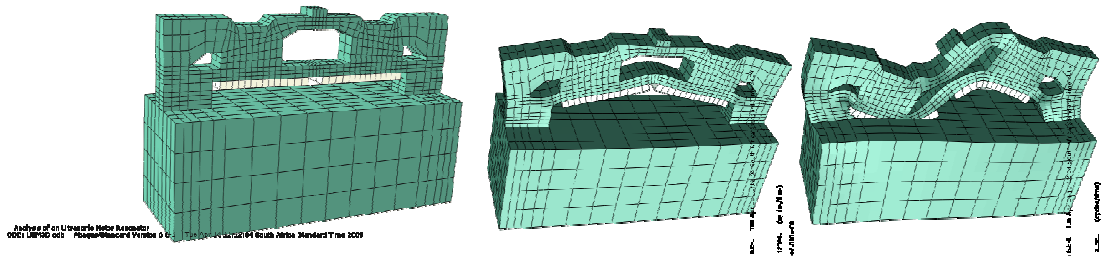

(a) **(b)** **(c)**

Figure 2: (a) Stator finite element mesh and mode shapes at (b) 10.867 and (c) 21.532 kHz

Figure 3 shows the motor test setup including the aluminium resonator, a slider (linear bearing) and a spring. The resonator consists of a 60 x 20 mm block of two different thicknesses (19.5 and 4.8 mm). Two polarised piezoceramics (18x5x1.68 m) are bonded within the bottom cavities, as indicated in figure 3(a). The spring exerts a normal force (*Fn*) between the steel slider and the contact point on the resonator.

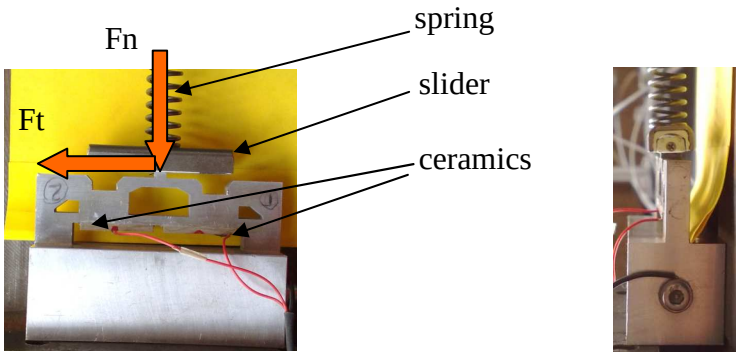

(a) (b)

Figure 3: Motor assembly test setup (a) front and (b) side views

4 Stator free vibration characterization using 3D scanning vibrometer

In order to characterise the stator, first the resonator was measured without the contacting slider. To experimentally identify the targeted resonator vibratory modes, a Polytec Scanning Vibrometer PSV 4000 was used, since it can scan an object and determine the vibratory motion of the individual surface points.

The output signal from the internal generator was linearly amplified using an AA LAB Systems Ltd A-303 High Voltage Amplifier and Modulator and used to drive the piezoceramic in the chosen frequency range of 8-40 kHz. The measured frequency response (figure 4 (b)) shows the two operating vibration modes at 10.4 and 20.525 kHz being in the expected ratio of about 1/2.

Table 1 presents the experimentally measured frequencies of the two modes of interest, together with the numerically predicted values. Although the measured values were accurately predicted (4% error) the ratio between the two frequencies was not adequate (.567). Therefore, the detailed finite element analysis (FEA) was used to iteratively tune the design such that the frequency ratio was acceptable. The stator was then machined as prescribed by the FEA and re-measured. The frequency ratio of 0.507 was achieved.

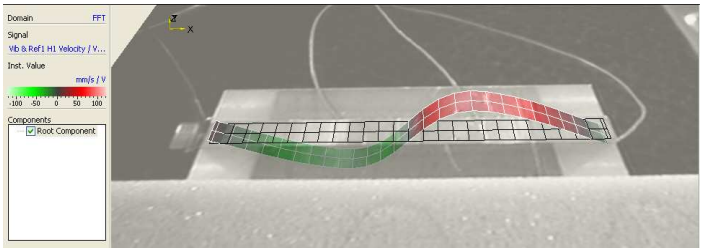

a) Operating deflection at 20.525 kHz

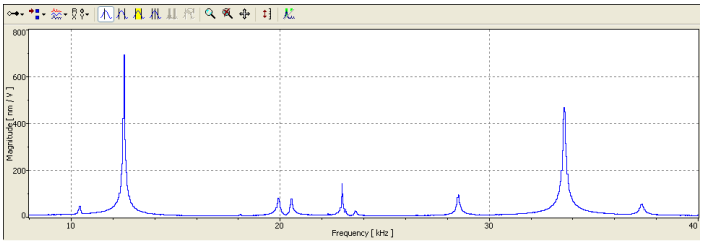

b) Frequency response

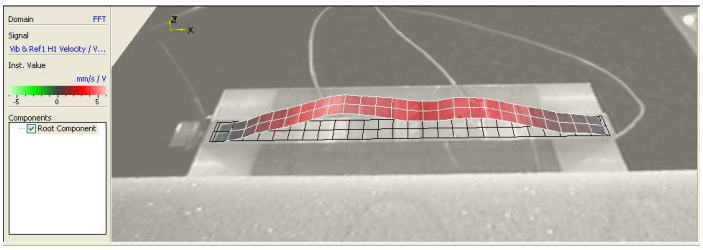

c) Operating deflection at 10.4 kHz

Figure 4: Resonator frequency response

Table 1: Experimental and theoretical frequency response

Experimental Pre machining	Experimental Post machining	FEM pre machining	FEM post machining
20.775 kHz	20.525 kHz	21.561 kHz	21.532 kHz
11.775 kHz	10.4 kHz	12.098 kHz	10.867 kHz

In order to plot the trajectory of the stator output point, both the normal (to the base) and the in-plane displacements of the output point are required. In its usual configuration, the laser vibrometer measures only the normal displacements and therefore the modified experimental setup depicted schematically in figure 5 was required.

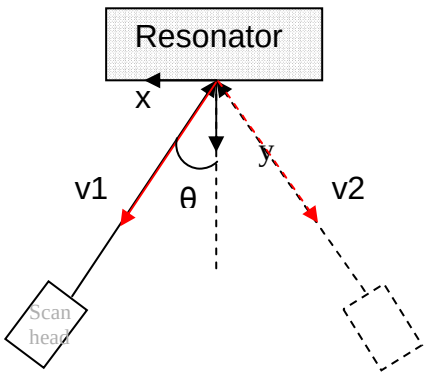

Figure 5: Setup to measure point normal and tangential velocity components

In this case, a driving signal containing the two targeted frequencies was generated using the Matlab Data Acquisition Toolbox. The velocity of the contact point, v_1, was then measured with the device at an angle $\theta = 30^0$ with respect to the beam as depicted in figure 5. The experiment was then repeated with $\theta = -30^0$ with resultant velocity v_2; a transformation eq.(3) is then used to determine the in-plane v_x and normal, v_y velocities.

$$\begin{bmatrix} v_x \\ v_y \end{bmatrix} = \begin{bmatrix} \sin\theta & \cos\theta \\ -\sin\theta & \cos\theta \end{bmatrix}^{-1} \begin{bmatrix} v_1 \\ v_2 \end{bmatrix} \tag{3}$$

In figures 6 (a) and (b) the measured signals $v_{i(i=1,2)}$ are presented. The computed in-plane and normal velocities v_x and v_y are plotted (figure 6 (c) and (d)). Finally the in-plane displacement is plotted against the normal displacement to yield the figure-of-eight trajectory in figure 6 (e).

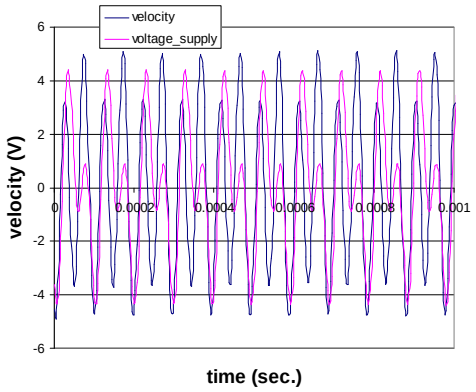

a) Signal v_1

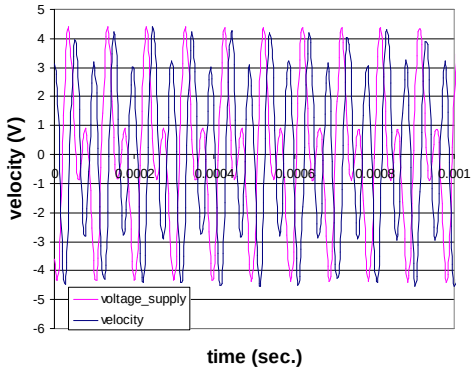

b) Signal v_2

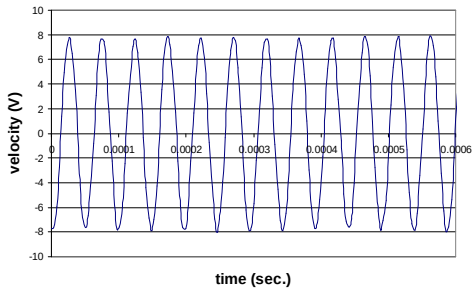

c) Signal v_x

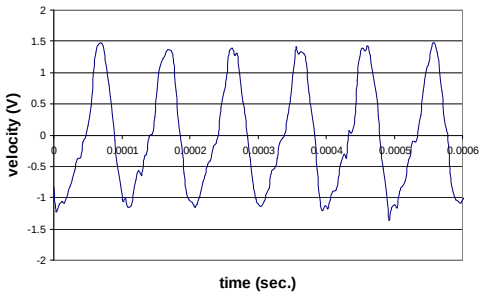

d) Signal v_y

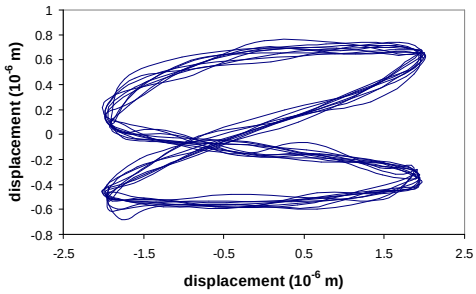

e) Figure-of-eight

Figure 6: Measured normal and tangential point velocity components and Figure-of-eight output trajectory

5 Mechanical characterisation of the motor assembly

Testing the motor involved adjusting the spring force and drive frequency to determine the maximum speed and force that could be achieved. Beforehand, the impedance curve from the prototype setup of the figure 7 gave a clue that only small contact force of the slider against the resonator was possible because the modes had been tuned to a frequency ratio of 1:2 with a free resonator. Indeed, the impact of a force against the contact point which results in a displacement of the first mode's resonant frequency as well as the diminution of the maximum magnitude of the displacement is seen. In fact, in the figure 7, the contact point is free of any load before being progressively loaded while the displacement of an accessible point of the surface containing the contact point is measured around 10.4 kHz. The measurements were carried out using a HP 3563A Control Systems Analyser.

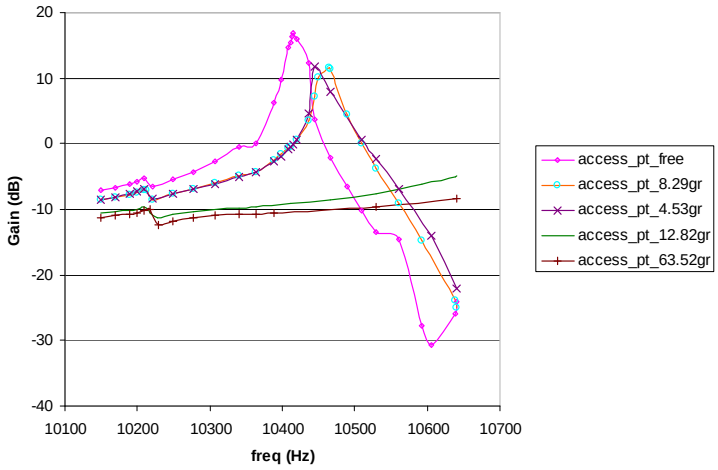

Figure 7: Device frequency response around 10.4 kHz

The developed prototype achieved a maximum measured slider speed of approximately 14 mm/s. The maximum force was determined by applying a gentle force against the slider through the spring. A maximum force of 50 mN was obtained. The maximum speed and force were obtained with different spring loads in open loop while the amplitude of the driving signal was 170 V.

6 Conclusion

We investigated the theoretical oscillating behaviour of a resonator, and confirmed its validity using experimental measurements of the output point. It was shown that at this contact point the resonator could produce the required figure-of-eight trajectory. Though the force and speed generated by the motor are still low, they are in the range of those developed by number of similar devices and can be improved.
A more advanced ultrasonic motor setup is currently under development and will be used in future to more fully and accurately measure the force and speed characteristics and their dependence on preload.

References

1. G. D. Gute and S.L. Hatler, Characterizing the Effects of Friction Liner Materials On The Performance of Piezoelectric Motors Using Finite Element Analysis, Kansas City Division, *KCP-613-5695*, Published October 1995.
2. K. Spanner, O. Vyshnevsky, W. Wischnewskiy, Design of Linear Ultrasonic Micro Piezo Motor for Precision Mechatronic Systems, in *Proceedings of the 10th International Conference on New Actuators (*Actuator 2006*)*, Bremen, Germany.
3. M. Fleischer, D. Stein, and H. Meixner, New Type of Piezoelectric Ultrasonic Motor, *IEEE Transactions on ultrasonics, ferroelectrics, and frequency control*, vol. 36. No.6. November 1989.
4. K. Uchino, Piezoelectric ultrasonic motors: overview**,** *Smart Mater. Struct.* **7** (1998) 273–285. Printed in the UK.
5. P. W. Loveday, C. S. Long, A. Groenwold, Ultrasonic Motor Resonator Design using Shape and Topology Optimisation, *Smart Structures and Materials 2004: Smart Structures and integrated Systems*, edited by Alison B. Flatau, Proc. Of SPIE Vol. 5390 (SPIE, Bellingham, WA, 2004).